Macromolecules

ARTICLE

pubs.acs.org/Macromolecules

Solid-State NMR Study of Stereocomplexes Formed by Enantiomeric Star-Shaped PEG−PLA Copolymers in Water

Lucia Calucci,*[,†] Claudia Forte,[†] Sytze J. Buwalda,[‡] and Piet J. Dijkstra[‡]

[†]Istituto di Chimica dei Composti OrganoMetallici, CNR-Consiglio Nazionale delle Ricerche, Area della Ricerca di Pisa, via G. Moruzzi 1, 56124, Pisa, Italy

[‡]Department of Polymer Chemistry and Biomaterials, Faculty of Science and Technology, MIRA Institute for Biomedical Technology and Technical Medicine, University of Twente, P.O. Box 217, 7500 AE Enschede, The Netherlands

ABSTRACT:

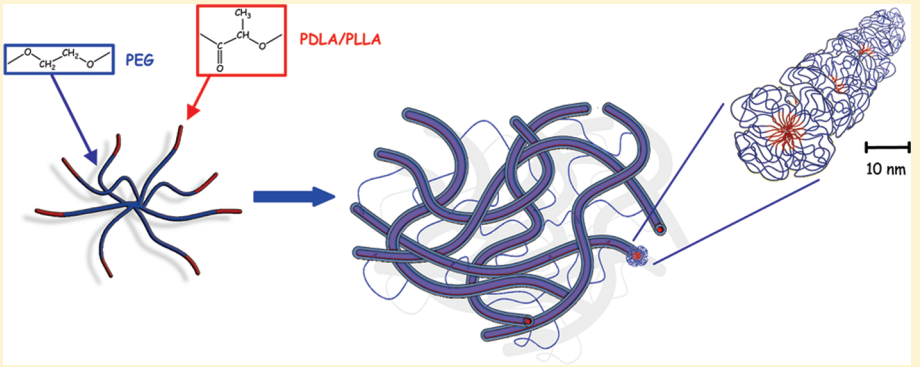

Solid-state NMR was applied to samples obtained by freeze-drying hydrogels of 1:1 $(PEG_{65}\text{-}NHCO\text{-}PLLA_{13})_8/(PEG_{65}\text{-}NHCO\text{-}PDLA_{13})_8$ or $(PEG_{65}\text{-}NHCO\text{-}PDLA_{13})_8$ only star block copolymers (where PEG, PLLA, and PDLA stand for poly(ethylene glycol), poly(L-lactide), and poly(D-lactide), respectively) in order to get insight into the different structural and dynamic properties of stereocomplexed poly(lactide) (PLA) aggregates with respect to single enantiomer ones responsible for the improved mechanical and degradation properties of the corresponding hydrogels. ^{13}C MAS NMR experiments together with ^{13}C relaxation time measurements indicated that the PLA domains in $(PEG_{65}\text{-}NHCO\text{-}PLLA_{13})_8/(PEG_{65}\text{-}NHCO\text{-}PDLA_{13})_8$ were highly crystalline, whereas those in $(PEG_{65}\text{-}NHCO\text{-}PDLA_{13})_8$ were mainly amorphous. On the basis of ^1H relaxation and spin-diffusion experiments, similar average dimensions were determined for the PLA aggregates in the two samples. PLA stereocomplexation was found to strongly affect the conformational behavior of PEG chains. Under the assumption that freeze-drying preserves the structure of at least the PLA aggregates, the results obtained are of value for understanding self-aggregation of PEG−PLA star block copolymers in water.

INTRODUCTION

Copolymers of poly(lactide) (PLA) and poly(ethylene glycol) (PEG) have been extensively studied in the past decade for their potential biomedical applications as scaffolds in tissue engineering and as drug delivery systems thanks to their nontoxicity, biocompatibility, and biodegradability.[1] Physically cross-linked PEG−PLA hydrogels can be formed by the self-assembling of di- and triblock copolymers driven by the association of the hydrophobic PLA blocks into micellar structures. These hydrogels usually show high water content, surface tension, and transport properties of cell metabolites similar to those of tissues. On the other hand, their mechanical properties not always match those of the target native tissue. This is in some cases regarded as a drawback because the overall mechanical environment affects cell proliferation and growth.

It has been reported that the stiffness of AB and ABA type hydrogels made from copolymers of PLA (A) and PEG (B) can be modified by controlling the degree of polymerization and the stereochemistry of the PLA blocks, since crystalline domains formed by optically pure PLA blocks lead to less labile junctions in the network with respect to amorphous domains of racemic PLA.[1,2] Moreover, the release rate of hydrophobic drugs from PLA−PEG−PLA micelles has been found to mainly depend on PLA block length and crystallinity.[3] Stereocomplexation, i.e., cocrystallization, of poly(L-lactide) (PLLA) and poly(D-lactide) (PDLA) blocks has also been exploited to introduce stable cross-links and, thereby, improve the mechanical properties of hydrogels formed by PEG−PLA diblock,[4−10] triblock,[4,10−14] and star block[14−18] copolymers.[19] Furthermore, it has been shown that enantiomeric PEG−PLA star block copolymers with a central PEG core and outer PLA blocks gelate faster and form

Received: May 26, 2011
Revised: July 14, 2011
Published: August 24, 2011

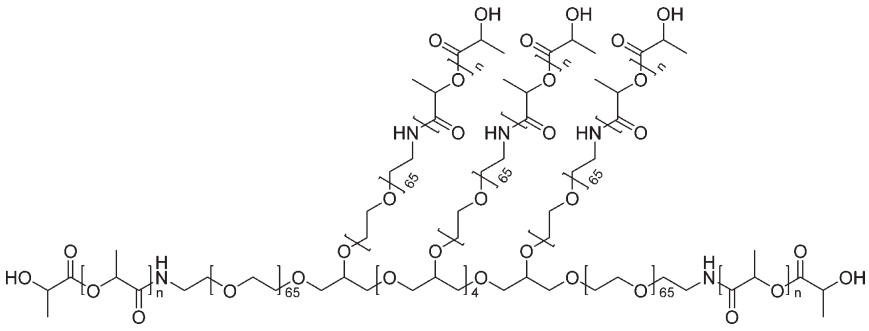

Figure 1. Molecular structure of the $(PEG_{65}\text{-NHCO-PLA}_n)_8$ star block copolymers.

stereocomplexed hydrogels with improved mechanical strength as compared to triblock copolymers.[14,15]

Stereocomplexes of 8-armed PEG−PLA star block copolymers linked by an amide group between the PEG core and the PLA arms ($(PEG_{65}\text{-NHCO-PLA}_n)_8$ with n = 11 and 13 in Figure 1) were recently prepared by our group, and their aggregation behavior in water was characterized.[18] These materials were found to form gels at significantly lower polymer concentration in comparison with the corresponding copolymers containing PLA single enantiomers, displaying higher storage moduli and stability to degradation *in vitro*. These properties were related to a higher rigidity of the stereocomplexed hydrophobic PLA aggregates constituting the gel cross-links with respect to single enantiomer ones, as indirectly revealed by solution-state ^{1}H nuclear magnetic resonance (NMR) spectroscopy. In fact, in heterogeneous systems, as hydrogels are, this technique allows water and the more mobile polymer components to be investigated, the rigid polymer moieties being pinpointed by the absence of the corresponding resonances. Solid-state NMR techniques, which have demonstrated of value for the characterization of complex systems thanks to their ability to selectively detect structurally and dynamically different environments, cannot be fully exploited for the investigation of rigid aggregates in hydrogels due to the usually low polymer concentration and the limitations to fast sample rotation imposed by the presence of large quantities of water.

The aim of the present work was a detailed molecular-level characterization of the crystallinity and dynamics of PLA aggregates in 8-armed PEG−PLA star block copolymers, trying to understand the influence of stereocomplexation on these properties, which are indicative of the aggregation behavior in the gel state. To this end, solid-state NMR spectroscopy and relaxation experiments were applied to solid samples obtained by freeze-drying stereocomplexed (1:1 mixture of $(PEG_{65}\text{-NHCO-PLLA}_{13})_8$/$(PEG_{65}\text{-NHCO-PDLA}_{13})_8$) or single enantiomer hydrogels ($(PEG_{65}\text{-NHCO-PDLA}_{13})_8$ (Figure 1, with n = 13), where the freeze-drying process was assumed to preserve at least the PLA aggregate structure from the gel to the solid state. In particular, ^{13}C cross-polarization (CP) and direct excitation (DE) magic angle spinning (MAS) experiments were combined to highlight copolymer moieties with different mobility and structure. Moreover, ^{1}H longitudinal relaxation times in the laboratory (T_1) and in the rotating ($T_{1\rho}$) frame, ^{13}C T_1's, and ^{1}H−^{13}C cross-polarization times (T_{CH}) were determined for the different groups of the copolymer chains exploiting the high resolution of ^{13}C spectra. Proton T_1 and $T_{1\rho}$ relaxation times, affected by spin diffusion, were used to get information on the structural heterogeneity. On the other hand, ^{13}C T_1 and T_{CH} values gave indications on the degree of mobility of the different groups giving a resolved ^{13}C NMR signal. A quantitative determination of the structural heterogeneity and dimensions of PEG and PLA domains was possible through spin-diffusion experiments,[20−22] where the time dependence of the redistribution of magnetization in space from mobile to rigid components was measured. On the basis of the results obtained and assuming the wormlike micellar structure observed for analogous copolymers by cryo-TEM analyses,[15] the PLA domains could be depicted as cylinders with a diameter of about 9 nm surrounded by a few nanometers thick corona of amorphous PEG, with crystalline PEG filling the interaggregate space.

EXPERIMENTAL SECTION

Materials. Hydroxyl-terminated 8-armed poly(ethylene glycol) (PEG-$(OH)_8$, $M_{n,NMR}$ = 23700 g/mol) was purchased from Jenkem (Allen, TX) and purified before use by dissolution in dichloromethane and precipitation in cold diethyl ether. The PEG-$(OH)_8$ was converted into PEG-$(NH_2)_8$ as previously described.[23] L-Lactide and D-lactide were obtained from Purac (Gorinchem, The Netherlands) and used as received. The 8-armed poly(ethylene glycol)−poly(L-lactide) and poly(ethylene glycol)−poly(D-lactide) star block copolymers ($(PEG_{65}\text{-NHCO-PLLA}_{13})_8$ and $(PEG_{65}\text{-NHCO-PDLA}_{13})_8$) were synthesized by the PEG-$(NH_2)_8$ initiated ring-opening polymerization of L-lactide and D-lactide, respectively, in toluene at 110 °C, as described in ref 18.

Samples for NMR measurements were prepared by dissolving $(PEG_{65}\text{-NHCO-PDLA}_{13})_8$ or a 1:1 mixture of $(PEG_{65}\text{-NHCO-PLLA}_{13})_8$ and $(PEG_{65}\text{-NHCO-PDLA}_{13})_8$ in distilled water at a concentration of 12% w/v, resulting in a single enantiomer hydrogel or a stereocomplexed hydrogel, respectively. Water was subsequently removed by freeze-drying at −50 °C and 5 × 10^{-7} bar.

PLLA and PDLA homopolymers ($M_{n,NMR}$ = 23 and 18 kg/mol, respectively) were prepared by the stannous octoate catalyzed ring-opening polymerization of L-lactide and D-lactide, respectively, in toluene at 110 °C using benzyl alcohol as an initiator. The reactions were allowed to proceed for 4 h in a nitrogen atmosphere. The mixtures were filtered and concentrated under reduced pressure. PLLA and PDLA were purified by precipitation in a 20-fold excess of a mixture of cold diethyl ether and methanol (20/1 v/v), obtained by filtration and dried overnight in vacuo at room temperature. Stereocomplexes of PLLA and PDLA were prepared by a precipitation method previously described.[24] Briefly, PLLA and PDLA solutions in dichloromethane (0.2 g/mL) were mixed, and the resulting solution was precipitated in a 20-fold excess of cold diethyl ether. The PLLA/PDLA stereocomplex was obtained by filtration and dried overnight in vacuo at room temperature.

DSC Measurements. DSC measurements were performed using a Mettler Toledo Star-e SW system with heating and cooling rates of 10 °C/min. Samples were heated from −70 to 250 °C and then cooled

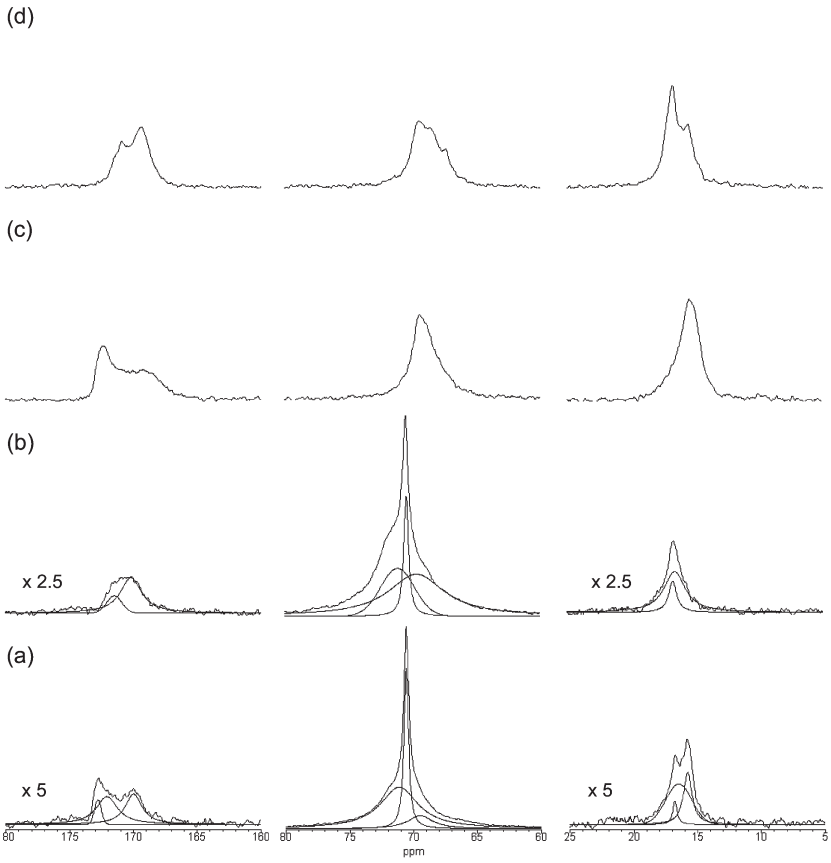

Figure 2. Expanded regions of interest of the ^{13}C DE MAS NMR spectra of (a) the PEG−PDLA/PEG−PLLA stereocomplex, (b) PEG−PDLA, (c) the PDLA/PLLA stereocomplex, and (d) PDLA. The spectra were recorded with a recycle delay of 120 s, accumulating 1200 scans. For the spectra of PEG−PDLA/PEG−PLLA and PEG−PDLA signal deconvolution is also shown.

to −70 °C, kept at −70 °C for 5 min, and heated again to 250 °C. Crystallization temperatures (T_c) were obtained from the cooling scan, while melting temperatures (T_m) were obtained from the second heating scan.

Solid-State NMR Experiments. NMR experiments were carried out on a Bruker AMX-300 WB spectrometer working at 300.13 MHz for proton and at 75.47 MHz for carbon-13.

^{13}C MAS NMR spectra were recorded under proton decoupling conditions using a 4 mm CP MAS probe head for solid-state measurements. The MAS frequency was 6 kHz. All experiments were performed at 20 °C; the temperature was controlled within 0.1 °C.

In the ^{13}C DE experiments the 90° pulse length was 4 μs, and recycle delays of 6 and 120 s were used in order to select spectral components with different ^{13}C longitudinal relaxation times. The number of scans acquired ranged from 600 to 2000 depending on the experiment.

In the $^{1}H-^{13}C$ CP experiments, the ^{1}H 90° pulse length was 4 μs and the spin-lock field was 62.5 kHz. Contact time (t_{CP}) values of 500 μs and 2 ms were used for recording CP MAS spectra. Delayed CP spectra were recorded using a 30 μs delay prior to the contact pulse (t_{CP} = 2 ms). In both CP and delayed CP experiments the recycle delay was 5 s, and 2000 scans were acquired. Variable contact time CP experiments were performed with t_{CP} values ranging from 20 μs to 90 ms for the $(PEG_{65}\text{-}NHCO\text{-}PDLA_{13})_8/(PEG_{65}\text{-}NHCO\text{-}PLLA_{13})_8$ sample and from 20 μs to 40 ms for the $(PEG_{65}\text{-}NHCO\text{-}PDLA_{13})_8$ sample; 200 scans were acquired for each experiment.

^{1}H spin−lattice relaxation times in the laboratory frame (T_1) were measured using an inversion recovery pulse sequence through cross-polarization to ^{13}C (t_{CP} = 1 ms).[25] The recycle delay was 5 s, and 400 scans were acquired for each experiment; at least 20 different values for the variable delay were used for each sample.

^{1}H spin−lattice relaxation times in the rotating frame ($T_{1\rho}$) were measured at a rf field of 62.5 kHz through ^{13}C observation using a variable spin-lock time followed by CP with a t_{CP} of 1 ms;[26] at least 20 different spin-lock time values were used for each sample. The recycle delay was 5 s, and 200 scans were acquired for each experiment.

^{13}C spin−lattice relaxation times in the laboratory frame (T_1) were measured using the Torchia pulse sequence[27] with t_{CP} = 1 ms and at least 25 variable delay values ranging from 10 μs to 50 s. The recycle delay was 5 s, and 400 scans were acquired for each experiment.

For ^{1}H spin-diffusion measurements a dipolar filter[20,21] was applied which destroys the magnetization of the proton rigid phase in a manner very similar to a classical Goldman−Shen experiment.[28] Two repeating cycles of the dipolar filter with an interpulse delay of 10 μs were used. Mixing time (t_{mix}) values ranging from 200 μs to 100 ms were employed. The resulting ^{1}H magnetization was detected through cross-polarization in ^{13}C CP MAS spectra; a CP contact time of 2 ms was used. The recycle delay was 5 s, and 2000 scans were acquired for each experiment.

NMR Data Analysis. NMR spectral deconvolution was performed by using the SPORT-NMR software,[29] using Lorentzian or Gaussian line shapes. The peak areas determined at different values of the characteristic sequence delays were used to determine spin−lattice relaxation times from fittings performed in terms of the appropriate functions. In particular, an exponential function was used to determine ^{1}H $T_{1\rho}$ and ^{13}C T_1 values from data of variable spin-lock and Torchia

Figure 3. ^{13}C MAS NMR spectra of PEG−PDLA (left) and PEG−PDLA/PEG−PLLA (right): (a) DE spectra acquired with a recycle delay of 120 s and 600 scans; (b) DE spectra acquired with a recycle delay of 6 s; (c) delayed CP spectra acquired with t_{CP} = 2 ms preceded by a 30 μs delay; (d) CP spectra acquired with t_{CP} = 2 ms; (e) CP spectra acquired with t_{CP} = 500 μs. In (b)−(d) 2000 scans were acquired. The spinning rate was 6 kHz.

experiments, respectively. ^{1}H T_1 values were determined by fitting the inversion recovery curve using the equation

$$I(t) = I_\infty(1 - \alpha \exp(-t/T_1)) \quad (1)$$

where I_∞ is the signal intensity at time ∞ and α is a parameter accounting for noncomplete magnetization inversion.[30] ^{1}H−^{13}C cross-polarization times (T_{CH}) were determined by fitting the data acquired in variable contact time experiments to the equation[26]

$$I(t) = \frac{I(0)}{T_{CH}} \frac{\exp(-t/T_{1\rho}(H)) - \exp(-t/T_{CH})}{\frac{1}{T_{CH}} - \frac{1}{T_{1\rho}(H)}} \quad (2)$$

where the ^{1}H $T_{1\rho}$ values were those determined from variable spin-lock experiments.

RESULTS AND DISCUSSION

^{13}C MAS NMR Spectra: Degree of Crystallinity. In order to investigate the structural and dynamic properties of the PEG and PLA chains in the $(PEG_{65}\text{-NHCO-PDLA}_{13})_8/(PEG_{65}\text{-NHCO-PLLA}_{13})_8$ stereocomplex (in the following indicated as PEG−PDLA/PEG−PLLA) and in $(PEG_{65}\text{-NHCO-PDLA}_{13})_8$ (in the following PEG−PDLA), ^{13}C CP and DE MAS experiments were recorded at 20 °C under different experimental conditions on both samples; representative spectra are shown in Figures 2 and 3. In particular, components with different mobility were distinguished by comparing DE spectra with short and long recycle delay, the former displaying only the more mobile components; on the other hand, the rigid components were highlighted by CP MAS experiments using appropriate contact time (t_{CP}) values. The DE MAS spectra acquired with a long recycle delay (120 s), which can be considered quantitative for all carbon signals except for the carbonyl carbon in the stereocomplex (see ^{13}C T_1 values reported below), were used for the assignment of the different signals to PEG and PLA chain moieties in amorphous and crystalline domains. The assignment of the PLA signals was supported by the comparison of the PEG−PLA copolymer spectra with those of purpose-made samples (see Experimental Section) of a PDLA homopolymer (Figure 2d) and a stereocomplex between PDLA and PLLA homopolymers (Figure 2c), also taking into account the assignment of solid-state ^{13}C NMR spectra previously reported in the literature for several samples of poly(L-lactide),[31] PLLA/PDLA stereocomplex,[32] and PEG[33,34] with different degrees of crystallinity.

In the spectra of PDLA and PDLA/PLLA (Figures 2d and 2c, respectively) signals typical of semicrystalline samples were observed,[31,32] with the PDLA/PLLA spectrum showing a carbonyl peak at 172.5 ppm peculiar of the crystalline stereocomplex phase. In the PEG−PDLA spectrum (Figure 2b) broad signals centered at about 16.7 and 170.9 ppm were observed for the PDLA methyl and carbonyl carbons, respectively, ascribable to mainly amorphous PDLA chains on the basis of deconvolution results.[31] On the other hand, the PEG−PDLA/PEG−PLLA sample showed three peaks in the methyl spectral region (16.8, 16.5, and 15.8 ppm) and three in the carbonyl spectral region (172.8, 171.5, and 170.0 ppm), as highlighted by the spectral deconvolution shown in Figure 2a. On the basis of the signal assignment reported in the literature,[32] the methyl peak at 15.8 ppm and the carbonyl peak at 172.8 ppm were attributed to the PDLA/PLLA stereocomplex crystalline phase, while the methyl signals at 16.8 and 16.5 ppm and the carbonyl signals at 171.5 and 170.0 ppm could be ascribed to crystalline and amorphous PLLA or PDLA chains, respectively.

In the spectra of PEG−PDLA/PEG−PLLA and PEG−PDLA (Figures 2a and 2b) the signals of PEG methylene and PLA methine carbons overlapped. The application of a spectral deconvolution procedure allowed three distinct peaks to be assigned (see Figure 2a); a narrow peak at 70.5 ppm and a broad peak at 71.1 ppm were ascribed to amorphous and crystalline PEG chains, respectively, in agreement with the literature,[33,34] whereas a peak at 69.5 ppm was attributed to PLA. From the relative intensities of the two PEG peaks it was found that 84 ± 5% and 61 ± 5% of the PEG chains are in a crystalline state in the PEG−PDLA and PEG−PDLA/PEG−PLLA sample, respectively.

The results obtained from the ^{13}C DE MAS NMR spectra were in agreement with those obtained from differential scanning calorimetry (DSC) experiments. In fact, both PEG−PDLA and PEG−PDLA/PEG−PLLA showed a transition at about 42 °C, corresponding to the melting of crystalline PEG, whereas a peak ascribable to the melting of PLA crystalline domains was observed in the second heating scan at 163.4 °C only for the stereocomplex sample.

The ^{13}C DE MAS NMR spectra acquired with short (6 s) and long (120 s) recycle delays on PEG−PDLA and PEG−PDLA/PEG−PLLA showed PLA methyl and PEG methylene signals with the same relative intensities, irrespective of the recycle delay employed. On the other hand, the PLA methine and carbonyl signals had lower intensity in the short recycle delay spectra, the

Table 1. ^{1}H T_1 and $T_{1\rho}$ Values, T_{CH} Values, and ^{13}C T_1 Values Determined for the PEG−PDLA/PEG−PLLA and PEG−PDLA Samples at 293 K

	PEG−PDLA				PEG−PDLA/PEG−PLLA			
relaxation time	CH_3	CH	$CH_{2amorphous}$	$CH_{2crystalline}$	CH_3	CH	$CH_{2amorphous}$	$CH_{2crystalline}$
$T_1(^1H)$ (ms)	735 ± 50	800 ± 70	720 ± 50	750 ± 50	560 ± 25	600 ± 50	580 ± 40	520 ± 30
$T_{1\rho}(^1H)$ (ms)	6.7 ± 0.4	5.9 ± 0.5	6.1 ± 0.2	0.7 ± 0.1	16 ± 2	16 ± 1	13 ± 1	0.4 ± 0.1
$T_1(^{13}C)$ (s)	0.71 ± 0.06	20 ± 5	0.19 ± 0.03	0.3 ± 0.1	0.92 ± 0.15	32 ± 5	0.21 ± 0.07	0.33 ± 0.03
T_{CH} (ms)	0.095 ± 0.014	0.2[a]	0.95 ± 0.09	0.046 ± 0.009	0.072 ± 0.009	0.20 ± 0.04	2.5 ± 0.3	0.054 ± 0.007

[a] Fixed in the fitting procedure to the value giving the best fitting results.

highest reduction being observed for the carbonyl peaks at 171.5 and 172.8 ppm in the stereocomplex spectrum (Figure 3a,b). For both PEG−PDLA and PEG−PDLA/PEG−PLLA samples the ^{13}C CP MAS spectra, acquired with contact times of 500 μs and 2 ms, showed enhanced relative intensities of the PLA peaks with respect to the overall intensity of the PEG signal (Figure 3a,c,d). Moreover, for the stereocomplex, a much higher proportion of the methyl and carbonyl peaks ascribed to stereocomplexed PLA chains was observed in the CP with respect to the DE spectra. In the CP MAS spectra acquired with shorter t_{CP} (500 μs), the PEG crystalline signal was enhanced with respect to the amorphous one, whereas the opposite occurred in the spectra acquired with longer t_{CP} (2 ms). Furthermore, the PEG crystalline component was practically absent when a 30 μs delay was introduced in the pulse sequence before cross-polarization (Figure 3c). For the stereocomplex, the delayed CP spectrum also showed a dramatic reduction of the PLA methyl and carbonyl signals ascribed to stereocomplexed chains.

On the basis of the comparison between ^{13}C MAS spectra recorded with different experimental conditions, amorphous PEG chains represented the most mobile component in both samples. These findings, together with the lower fraction of crystalline PEG found by NMR spectroscopy and the quite lower PEG crystallization temperature determined by DSC for the PEG−PDLA/PEG−PLLA sample (−5.0 °C instead of 9.4 °C), pointed out the strong influence of the stereocomplexed PLA domains on the phase behavior of a significant PEG fraction. Moreover, the two investigated samples showed a remarkably different morphism as far as the PLA domains are concerned. In fact, already in the DSC measurements, a melting transition ascribable to PLA was observed (at 163.4 °C) only for the PEG−PDLA/PEG−PLLA sample, indicating the formation of crystalline domains in this sample. Indeed, in the ^{13}C MAS spectra of the stereocomplex, signals ascribable to crystalline stereocomplexed PLLA and PDLA chains as well as a minor component of crystalline single enantiomer chains were observed, whereas signals ascribable to amorphous PDLA were mainly detected for PEG−PDLA (Figure 2). These findings can be explained considering that cocrystallization of PDLA and PLLA chains in a stereocomplexed configuration can occur for chain lengths shorter than that required for crystallization of the single enantiomers, as found for hydrogels of PEG−PLA star block copolymers by WAXS measurements[15] and for PLA homopolymers by DSC measurements.[35] The formation of crystalline PLA domains also for non-stereocomplexed chains in the PEG−PDLA/PEG−PLLA sample is most probably favored by the concomitant stereocomplexation.

^{13}C and ^{1}H Relaxation Times: PEG and PLA Chain Dynamics. In order to get further insight into the dynamics of PEG and PLA chains, ^{13}C and ^{1}H relaxation times were analyzed. ^{13}C

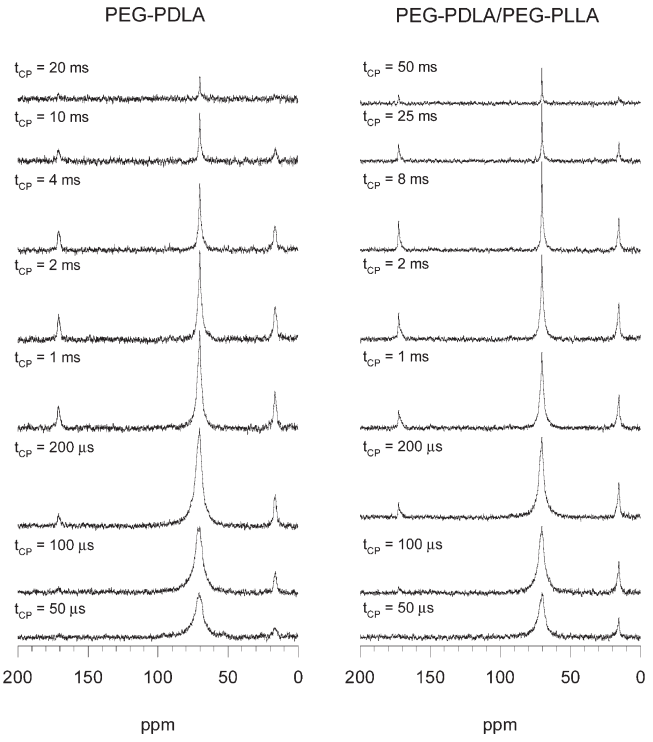

Figure 4. ^{13}C CP MAS NMR spectra of PEG−PDLA and PEG−PDLA/PEG−PLLA recorded at different contact time (t_{CP}) values.

T_1 relaxation times were determined using the Torchia pulse sequence[27] for both the PEG−PDLA and the PEG−PDLA/PEG−PLLA samples; the obtained values are reported in Table 1. T_1 values on the order of few hundreds of milliseconds were found for amorphous and crystalline PEG carbons with no significant differences between the two samples. On the other hand, T_1 values on the order of tens of seconds were determined for PLA carbonyl (23 ± 3 and 48 ± 7 s for PEG−PDLA and PEG−PDLA/PEG−PLLA, respectively) and methine (Table 1) carbons, with longer values in the case of the stereocomplex with respect to the PEG−PDLA sample. Also, the PLA methyl carbons, displaying much smaller values, showed slightly longer T_1 values for the stereocomplex with respect to the PEG−PDLA sample. Although ^{13}C T_1's are not straightforwardly interpretable in terms of dynamic parameters, the values obtained for PLA gave a clear indication of the higher degree of mobility of the PLA chains in PEG−PDLA with respect to PEG−PDLA/PEG−PLLA.

The degree of rigidity can be monitored also by measuring ^{1}H−^{13}C cross-polarization times (T_{CH}), these being typically very short for protonated carbons in highly rigid environments.

$^1H-^{13}C$ T_{CH} values were determined for the different PEG and PLA components by recording ^{13}C CP MAS experiments at different t_{CP} values on both the PEG−PDLA/PEG−PLLA and PEG−PDLA samples; a selection of spectra is shown in Figure 4. At very short contact times (<200 μs) all PLA peaks were observed, whereas only the broad crystalline PEG signal was detected. On the other hand, at long contact times (>4 ms) only the narrow amorphous PEG signal remained together with the PLA peaks, with a progressive decrease with increasing t_{CP}. Peak intensities determined from spectral deconvolution at different contact times were employed to calculate the $^1H-^{13}C$ T_{CH} values assuming ^1H $T_{1\rho}$ values determined from variable spin-lock experiments (vide infra); the obtained T_{CH} values are reported in Table 1.

PEG methylene groups in crystalline domains showed the shortest T_{CH} values (∼50 μs), with insignificant differences between the PEG−PDLA/PEG−PLLA and the PEG−PDLA sample. On the other hand, PEG methylene groups in amorphous chains showed the longest T_{CH} values in both samples, with longer values in the PEG−PDLA/PEG−PLLA sample (2.5 ms) with respect to the PEG−PDLA one (∼1 ms). As far as PLA carbons are concerned, increasing trends of T_{CH} values, compatible with the number of directly bonded protons, were found for methyl and methine groups.

^1H T_1 and $T_{1\rho}$ relaxation times were determined for PEG−PDLA and PEG−PDLA/PEG−PLLA from suitable ^{13}C CP MAS experiments[25,26] exploiting the resolution of ^{13}C spectra; the obtained values are reported in Table 1. Very similar T_1 values were found for all protons within the same sample, with shorter values in the case of the stereocomplex. For crystalline PEG chains a $T_{1\rho}$ value on the order of several hundreds of microseconds was found in both PEG−PDLA and PEG−PDLA/PEG−PLLA; on the other hand, all the other protons showed very similar $T_{1\rho}$ values in each sample, that is, ∼6 and ∼15 ms in the case of PEG−PDLA and of PEG−PDLA/PEG−PLLA, respectively. These data are evidence of the strong influence of spin diffusion on the measured relaxation times; hence, although they could not be used to obtain pure dynamic information, they were exploited to estimate average dimensions of PEG and PLA domains. Considering that T_1 and $T_{1\rho}$ of the different components can be averaged by spin diffusion over characteristic distances,[36] these findings indicate that amorphous PEG and PLA domains have average dimensions on the order of few nanometers, whereas crystalline PEG domain dimensions are larger, but certainly smaller than 50 nm. This maximum dimension is, on the other hand, compatible with the copolymer molecular architecture and chain length. The averaged longer $T_{1\rho}$ and shorter T_1 values found for the PEG−PDLA/PEG−PLLA sample with respect to the PEG−PDLA one are ascribable to the different intrinsic relaxation times in the PDLA/PLLA and PDLA domains, as suggested by relaxation time measurements on homopolymer samples. In fact, ^1H T_1 and $T_{1\rho}$ relaxation times of 500 ± 50 and 56 ± 5 ms and of 780 ± 50 and 38 ± 5 ms were measured by us for purposely made PDLA/PLLA stereocomplex and PDLA homopolymer, respectively.

Spin Diffusion: Aggregate Morphology. A more accurate determination of domain sizes could be obtained by investigating the ^1H spin-diffusion process on both the PEG−PDLA/PEG−PLLA and PEG−PDLA samples. To this end, the proton magnetization of the mobile amorphous PEG chains was selected on the basis of the longer spin−spin relaxation time by applying a dipolar filter, and the magnetization transfer to more rigid components, that is PLA chains and crystalline PEG chains, was monitored at different mixing times (t_{mix}) through ^{13}C detection by recording CP MAS spectra.[20−22] As shown in Figure 5, with increasing the t_{mix} value, signals from the PLA chains appeared in the spectrum and increased up to the equilibrium value, reached at $t_{mix} \cong 60$ ms for both the PEG−PDLA/PEG−PLLA and the PEG−PDLA samples. Correspondingly, the intensity of the amorphous PEG chains progressively decreased, reaching a plateau at the equilibrium value. On the other hand, the signal relative to crystalline PEG chains started to significantly increase

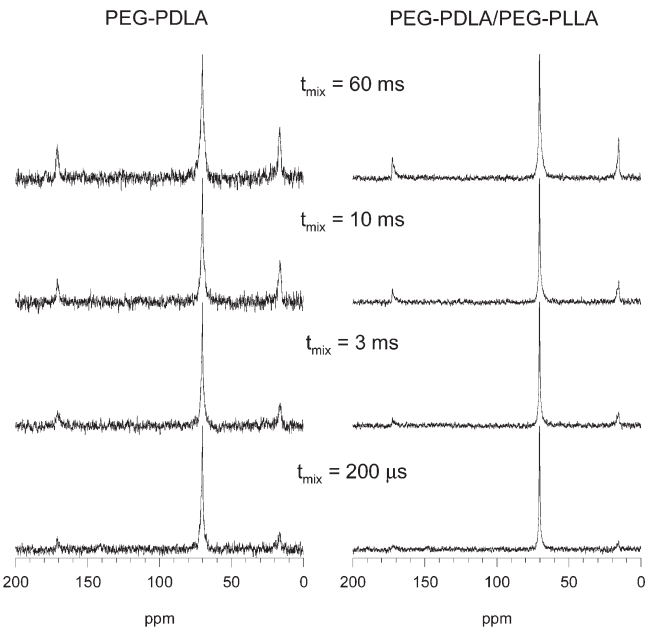

Figure 5. ^{13}C CP MAS NMR spectra of PEG−PDLA and PEG−PDLA/PEG−PLLA recorded at different t_{mix} values after selection of the amorphous PEG magnetization by application of a dipolar filter.

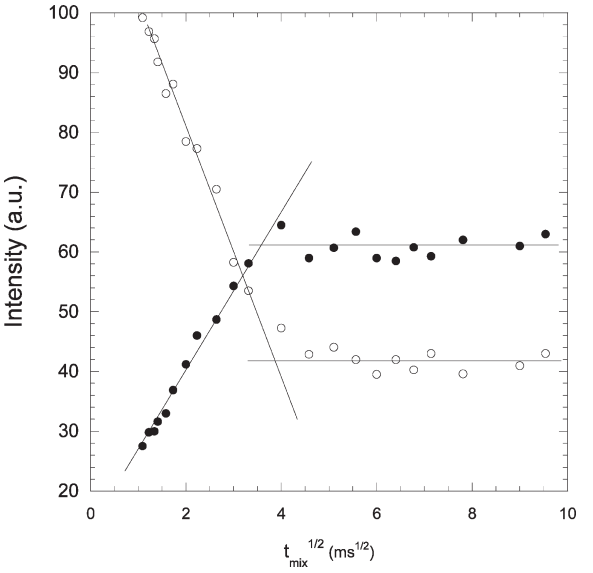

Figure 6. Integrated intensities of the PLA methine (full circles) and amorphous PEG methylene (empty circles) signals in ^{13}C CP MAS spectra of the PEG−PDLA sample recorded at different mixing times after the application of a dipolar filter.

Table 2. Parameters Used in eq 3 for the Calculation of Domain Sizes

parameter	PEG−PDLA	PEG−PDLA/PEG−PLLA
D_{PLA} (nm^2 ms^{-1})	0.21[42]	0.6
ρ_{HPLA} (g cm^{-3})	0.069	0.074
Φ_{PLA}	0.65	0.43

only at a mixing time of 80 ms when proton longitudinal relaxation starts to be effective.

For both samples, the intensities of PLA and amorphous PEG signals showed a linear trend with $(t_{mix})^{1/2}$ for small t_{mix} values, the former increasing and the latter decreasing correspondingly, as expected in the case of a two-phase system with a small interfacial thickness with respect to the size of the different domains.[21,22] The trend of the peak intensities for the PLA methine and amorphous PEG methylene signals in the PEG−PDLA sample is shown as an example in Figure 6.

The plots of the peak intensities of PLA methyl, methine, and carbonyl and of amorphous PEG signals were used to determine $(t^*_{mix})^{1/2}$, that is, the $(t_{mix})^{1/2}$ value corresponding to the intersection of the initial rate line with the equilibrium intensity value. Values of 3.8 ± 0.3 and 4.7 ± 0.3 $ms^{1/2}$ were determined for $(t^*_{mix})^{1/2}$ in the PEG−PDLA and PEG−PDLA/PEG−PLLA sample, respectively.

These $(t^*_{mix})^{1/2}$ values were employed to evaluate the PLA domain sizes (d_{PLA}) in the two investigated samples within the initial-rate approximation using the equation[21,22]

$$d_{PLA} = \frac{\rho_{HPEG}\Phi_{PEG} + \rho_{HPLA}\Phi_{PLA}}{\Phi_{PEG}\Phi_{PLA}} \frac{4\varepsilon\Phi_{PLA}}{\sqrt{\pi}} \times \frac{\sqrt{D_{PEG}D_{PLA}}}{\sqrt{D_{PEG}}\rho_{HPEG} + \sqrt{D_{PLA}}\rho_{HPLA}} \sqrt{t^*_{mix}} \quad (3)$$

where ρ_{Hi}, Φ_i, and D_i are the proton density, volume fraction, and spin-diffusion coefficient of phase i, respectively, and ε is the dimensionality of the phase structure. On the basis of the wormlike micellar structure observed for analogous systems by cryo-TEM analyses,[15] the PLA domains in the freeze-dried samples were considered as cylinders surrounded by an amorphous PEG corona; hence, ε was taken equal to 2. D_{PEG} = 0.1 nm^2 ms^{-1} and ρ_{HPEG} = 0.103 g cm^{-3} were considered for amorphous PEG,[37,38] while for the PLA phase the parameter values reported in Table 2 were used. The diffusion coefficients and proton densities were taken from the literature, except for the diffusion coefficient of the stereocomplexed PLA for which no value was reported and which was assumed 0.6 nm^2 ms^{-1} considering its high crystallinity.[39] The ρ_{HPLA} and Φ_{PLA} values were calculated on the basis of the sample stoichiometry and the densities determined for the different components.[40,41] Using the experimentally determined $(t^*_{mix})^{1/2}$ values, diameters of 9.0 ± 0.5 and 9.2 ± 0.5 nm were obtained for the PLA domains in PEG−PDLA and in the stereocomplex sample, respectively. The corresponding overall dimensions d for the PLA core and PEG corona, calculated using the following equation[22]

$$d = \frac{d_{PLA}}{\sqrt{\Phi_{PLA}}} \quad (4)$$

were found to be 11.2 ± 0.5 and 14.0 ± 0.5 nm, respectively. These dimensions are in agreement with those previously determined by TEM analyses on similar systems.[15] These results suggest that the wormlike aggregates are cylinders with an inner core of PLA, with a diameter on the order of twice the PLA chain length, and an outer corona made of amorphous PEG, with a thickness of 1−2 monomeric units; interaggregate space is filled by crystalline PEG, as sketched in Figure 7.

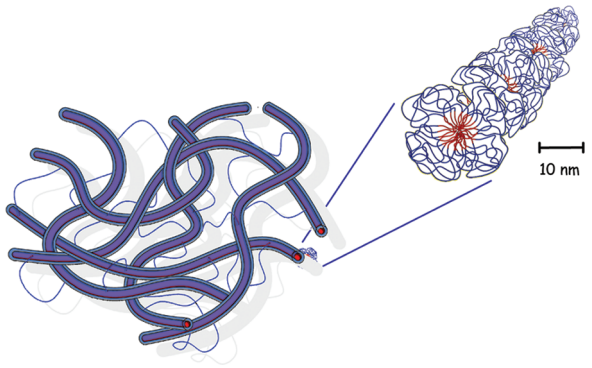

Figure 7. Sketch of the wormlike micellar structure of PEG−PDLA and PEG−PDLA/PEG−PLLA copolymers in the freeze-dried samples.

CONCLUSIONS

The application of solid-state NMR techniques to samples of 8-armed star block PEG−PDLA and PEG−PDLA/PEG−PLLA copolymers, prepared by freeze-drying hydrogels containing 12% w/v of polymer, gave valuable information for the interpretation of the hydrogel properties. In particular, the previously hypothesized formation of crystalline PLA domains by stereocomplexation of PEG−PDLA and PEG−PLLA in water was here clearly observed as opposed to the formation of amorphous PDLA aggregates in the PEG−PDLA system; the observed crystallinity can be associated with the high hydrogel stiffness and resistance to degradation by aggregate disruption previously found for the stereocomplexed systems.[18] The size of PLA aggregates, determined by spin-diffusion experiments, was found to be ∼9 nm, corresponding to approximately twice the length of an elongated PLA copolymer chain. The higher rigidity and density of the PLA stereocomplexed aggregates seems to impose constraints on the PEG chain conformational equilibrium disfavoring PEG crystallization, as indicated by the higher proportion and mobility of the amorphous PEG component found for the stereocomplex sample.

On the basis of the hydrophobic nature of poly(lactide), the findings regarding the crystallinity and morphology of PLA domains in the freeze-dried samples can be considered valid also for the corresponding hydrogels. On the other hand, the fraction of crystalline PEG in the freeze-dried samples most probably corresponds to PEG chains highly swollen in water in the hydrogels, which are the least affected by the PLA aggregation. On the contrary, the PEG fraction which is found amorphous in the solids represents in the hydrogel the PEG units surrounding the PLA domains, their conformational behavior being constrained by the PLA aggregation and more strongly in the case of stereocomplexation.

AUTHOR INFORMATION

Corresponding Author

*Phone +39-050-3152517; Fax +39-050-3152555; e-mail lucia.calucci@pi.iccom.cnr.it.

■ ACKNOWLEDGMENT

The authors thank Dr. E. Passaglia for performing DSC measurements.

■ REFERENCES

(1) Tew, G. N.; Sanabria-DeLong, N.; Agrawal, S. K.; Bhatia, S. R. *Soft Matter* **2005**, *1*, 253–258.
(2) Sanabria-DeLong, N.; Agrawal, S. K.; Bhatia, S. R.; Tew, G. N. *Macromolecules* **2006**, *39*, 1308–1310.
(3) Agrawal, S. K.; Sanabria-DeLong, N.; Coburn, J. M.; Tew, G. N.; Bhatia, S. R. *J. Controlled Release* **2006**, *112*, 64–71.
(4) Slager, J.; Domb, A. J. *Adv. Drug Delivery Rev.* **2003**, *55*, 549–583.
(5) Li, S. *Macromol. Biosci.* **2003**, *3*, 657–661.
(6) Li, S. M.; Vert, M. *Macromolecules* **2003**, *36*, 8008–8014.
(7) Li, S.; El Ghzaoui, A.; Dewinck, E. *Macromol. Symp.* **2005**, *222*, 23–35.
(8) Kang, N.; Perron, M.-È.; Prud'homme, R. E.; Zhang, Y.; Gaucher, G.; Leroux, J.-C. *Nano Lett.* **2005**, *5*, 315–319.
(9) Slager, J.; Brizzolara, D.; Cantow, H. J.; Domb, A. J. *Polym. Adv. Technol.* **2005**, *16*, 667–674.
(10) Tsuji, H. *Macromol. Biosci.* **2005**, *5*, 569–597.
(11) Lim, D. W.; Park, T. G. *J. Appl. Polym. Sci.* **2000**, *75*, 1615–1623.
(12) Kricheldorf, H. R.; Rost, S.; Wutz, C.; Domb, A. *Macromolecules* **2005**, *38*, 7018–7025.
(13) Bishara, A.; Kricheldorf, H. R.; Domb, A. J. *Macromol. Symp.* **2005**, *225*, 17–30.
(14) Hiemstra, C.; Zhong, Z.; Li, L.; Dijkstra, P. J.; Feijen, J. *Macromol. Symp.* **2005**, *224*, 119–131.
(15) Hiemstra, C.; Zhong, Z.; Li, L.; Dijkstra, P. J.; Feijen, J. *Biomacromolecules* **2006**, *7*, 2790–2795.
(16) Nagahama, K.; Nishimura, Y.; Ohya, Y.; Ouchi, T. *Polymer* **2007**, *48*, 2649–2658.
(17) Nagahama, K.; Fujiura, K.; Enami, S.; Ouchi, T.; Ohya, Y. *J. Polym. Sci., Part A: Polym. Chem.* **2008**, *46*, 6317–6332.
(18) Buwalda, S. J.; Dijkstra, P. J.; Feijen, J.; Calucci, L.; Forte, C. Manuscript in preparation.
(19) Fujiwara, T.; Yamaoka, T.; Kimura, Y. In *Biomedical Application of Hydrogels Handbook*, 1st ed.; Ottenbrite, R. M., Park, K., Okano, T., Eds.; Springer Science: New York, 2010; p 157.
(20) Egger, N.; Schmidt-Rohr, K.; Blümich, B.; Domke, W.-D.; Stapp, B. *J. Appl. Polym. Sci.* **1992**, *44*, 289–295.
(21) Schmidt-Rohr, K.; Clauss, J.; Blümich, B.; Spiess, H. W. *Magn. Reson. Chem.* **1990**, *28*, S3–S9.
(22) Clauss, J.; Schmidt-Rohr, K.; Spiess, H. W. *Acta Polym.* **1993**, *44*, 1–17.
(23) Elbert, D. L.; Hubbell, J. A. *Biomacromolecules* **2001**, *2*, 430–441.
(24) Tsuji, H.; Hyon, S.-H.; Ikada, Y. *Macromolecules* **1991**, *24*, 5657–5662.
(25) Kitamaru, R.; Horii, F.; Murayama, K. *Macromolecules* **1986**, *19*, 636–643.
(26) Stejskal, E. O.; Schaefer, J.; Sefcik, M. D.; McKay, R. A. *Macromolecules* **1981**, *14*, 275–279.
(27) Torchia, D. A. *J. Magn. Reson.* **1978**, *30*, 613–616.
(28) Goldman, M.; Shen, L. *Phys. Rev.* **1966**, *144*, 321–331.
(29) Geppi, M.; Forte, C. *J. Magn. Reson.* **1999**, *137*, 177–185.
(30) Gerhards, R.; Dietrich, W. *J. Magn. Reson.* **1976**, *23*, 21–29.
(31) Thakur, K. A. M.; Kean, R. T.; Zupfer, J. M.; Buehler, N. U.; Doscotch, M. A.; Munson, E. J. *Macromolecules* **1996**, *29*, 8844–8851.
(32) Tsuji, H.; Horii, F.; Nakagawa, M.; Ikada, Y.; Odani, H.; Kitamaru, R. *Macromolecules* **1992**, *25*, 4114–4118.
(33) Vanderhart, D.; Earl, W.; Garroway, A. *J. Magn. Reson.* **1981**, *44*, 361–401.
(34) Johansson, A.; Tegenfeldt, J. *Macromolecules* **1992**, *25*, 4712–4715.
(35) de Jong, S. J.; van Dijk-Wolthuis, W. N. E.; Kettenes-van den Bosch, J. J.; Schuyl, P, J. W.; Hennink, W. E. *Macromolecules* **1998**, *31*, 6397–6402.
(36) McBrierty, V. J.; Packer, K. J. *Nuclear Magnetic Resonance in Solid Polymers*; Cambridge University Press: Cambridge, UK, 1993; Chapter 6.
(37) Weigand, F.; Demco, D. E.; Blümich, B.; Spiess, H. W. *J. Magn. Reson., Ser. A* **1996**, *120*, 190–200.
(38) Buda, A.; Demco, D. E.; Bertmer, M.; Blümich, B.; Reining, B.; Keul, H.; Höcker, H. *Solid State NMR* **2003**, *24*, 39–67.
(39) Cai, W. Z.; Schmidt-Rohr, K.; Egger, N.; Gerharz, B.; Spiess, H. W. *Polymer* **1993**, *34*, 267–276.
(40) Sawai, D.; Tsugane, Y.; Tamada, M.; Kanamoto, T.; Sungil, M.; Hyon, S. H. *J. Polym. Sci., Part B: Polym. Phys.* **2007**, *45*, 2632–2639.
(41) Li, C. Y.; Birnkrant, M. J.; Natarajan, L. V.; Tondiglia, V. P.; Lloyd, P. F.; Sutherland, R. L.; Bunning, D. J. *Soft Matter* **2005**, *1*, 238–242.
(42) Jia, X.; Wang, X.; Tonelli, A. E.; White, J. L. *Macromolecules* **2005**, *38*, 2775–2780.